Rock Mechanics and Rock Engineering
https://doi.org/10.1007/s00603-024-04213-w

ORIGINAL PAPER

Experimental and Analytical Study on the External Water Pressure of a Composite Lining Considering the Waterproofing and Drainage System

Jinghui Liu[1,2] · Cagri Gokdemir[1] · Xiaojun Li[1] · Yue Xi[1]

Received: 14 June 2023 / Accepted: 5 October 2024

Abstract

Conventional analytical solutions for estimating the external water pressure neglect some factors associated with the waterproofing and drainage system (WDS), such as geotextile, circular drainage pipes, and waterproof membranes, which may lead to a gap between actual engineering observations and estimations. In this study, a reduced-scale model setup is designed to investigate the impact of the WDS on water pressure distributions. The model-test results indicate that the WDS dramatically reduces the water pressure on the secondary lining, while the effect on the initial lining is not apparent. An analytical solution is derived to analyze the external water pressure acting on the initial and secondary linings, and it is compared with model-test results. The results imply that the errors between the analytical solution and model test results ranged from −2.3% to 10.9%, thus verifying the proposed solution. Finally, a parametric analysis is conducted to reveal the WDS effect on water pressure. The following observations were made: (1) the external water pressure distribution acting on the initial and secondary linings is related to the distance between two adjacent circular drainage pipes, the surrounding rock mass and initial lining permeability, and the geotextile thickness. A small distance between the drainage pipes could increase water pressure reduction. (2) When the permeability coefficient of the surrounding rock mass is in the range of 1×10^{-8} to 5×10^{-6} m/s, the secondary lining water pressure prediction of the proposed solution is more than 54.1% lower than Liu's solution (Liu et al. 2013). The outcomes indicate the importance of the WDS effect on the water pressure under such conditions. This study results are helpful for the optimal design of composite lining structures and WDS.

Highlights

- A model test is designed to investigate the waterproofing and drainage system (WDS) effect on water pressure.
- An analytical water pressure solution on the initial and secondary lining is derived and validated.
- The components of the waterproofing and drainage systems (waterproof membranes, geotextile, and blind pipes) are considered.
- The changes of the water pressure acting on the secondary lining are more significant than those on the initial lining, as the distance between two adjacent circular drainage pipes increases.

Keywords Rock tunnel · Analytical solution · Water pressure · Waterproofing and drainage system · Model test

1 Introduction

External water pressure on the tunnel lining plays an essential role in the stability of tunnels (Zhou et al. 2015; Liu et al. 2019, 2023; Yang et al. 2021), and affects the tunnel safety

✉ Xiaojun Li
lixiaojun@tongji.edu.cn

[1] College of Civil Engineering, Tongji University, 1239 Siping Road, Shanghai 210098, China

[2] China Institute of Water Resources and Hydropower Research, 1Fuxing Road, Beijing 100038, China

Published online: 26 October 2024

during the operational stage (Jansson and Boström 2010; Preisig et al. 2014; Xu et al. 2019; Xie et al. 2019; Li et al. 2021a). The prediction of external water pressure, acting on the lining of water-rich mountain tunnels, is a critical and challenging issue in tunnel engineering (Gao and Qiu 2004; Ding et al. 2007; Bagnoli et al. 2015; Fang et al. 2016; Wei et al. 2020). Lining with smaller permeability could increase the external water pressure (Wang 2008; Xu et al. 2019; Yoo 2016; Li et al. 2019), while the tunnel drainage system would decrease the water pressure (Ponlawich et al. 2009). Various methods, such as analytical solutions (Park et al. 2008; Huangfu et al. 2010; Tang et al. 2018; Liu et al. 2020a; Fan et al. 2023), reduction coefficient methods (Zhang 2003; The Ministry of Water Resources of the People's Republic of China 2016), and numerical methods (Shin et al. 2009; Bian et al. 2009; Nikvar-Hassani et al. 2016; Golian et al. 2021; Zuo et al. 2022; Teng et al. 2023), have been proposed to predict the water pressure, acting on the lining. Comparing with numerical methods, analytical solutions are more practical and rapid (Parker et al. 2014; Maleki 2018). Thus, analytical solutions have been extensively used to predict the water pressure, because of their simplifications on mathematical theories (Farhadian and Katibeh 2015, Farhadian and Nikvar-Hassani 2018). The analytical solutions will be reviewed gradually based on the assumption of the drainage simplification in following text, that is, assuming single-layer lining drainage, two-layer lining drainage, and the WDS drainage respectively.

Early researchers have developed solutions based on the assumption that the groundwater uniformly penetrates the lining, and that the water pressure is exerted equally on the outer perimeter of the lining layer, neglecting the contributions of waterproof membranes and drainage pipes (Shin et al. 2007; Kolymbas and Wagner 2007; Ying et al. 2018; Wang et al. 2008; Zhou et al. 2014, Yang et al. 2014). Ying et al. (2018), Zhang (2006), and Yang et al. (2014) presented analytical solutions of water pressure with the assumption that a constant hydrostatic load is applied along the lining border. Wang et al. (2008) and Liu et al. (2023) investigated the distribution of water pressure on the lining using model tests and field measurements based on the assumption that the water pressure was equally applied at the lining's circumference. These solutions assumed that the composite lining was a single-layer lining. However, the composite tunnel lining contains an initial lining, a secondary lining, and a drainage system (Chen and liu 2023). Therefore, single-layer lining models cannot accurately predict the water pressure on the composite lining (He et al. 2015).

Some researchers assumed two-layered composite lining with uniformly penetrating groundwater pressure on the initial and secondary linings (Liu et al. 2013; Du et al. 2011; He et al. 2015). Other researchers have used the experimental model method to investigate the distribution of water pressure, in which the drainage pipes are considered (Zhao 2017, 2018; Zhang et al. 2022). For the sake of simplicity, these methods simplify the actual groundwater seepage path, and ignore the partial factors of the waterproofing and drainage system (WDS) (i.e., waterproof membranes, geotextiles, and blind pipes) on the water pressure. In practice, the groundwater is drained via blind pipes, instead of uniform seepage along the lining perimeter (Wang 2006; Chen and liu 2023). The seepage behavior is determined by the hydraulic boundary conditions and hydraulic properties of the materials involved in the seepage routes, such as the ground, lining, and drainage system (Shin et al. 2009; Zhang et al. 2011, 2022). Thus, the simplification mentioned above usually induces a significant gap between the existing solutions and actual situations (He et al. 2015). However, to the best of the authors' knowledge, no method has been published previously in the literature considering the entire WDS that follows the actual seepage path to calculate the water pressure. In addition, a few solutions exist that allow the exploration of the effect of the entire WDS on the water pressure.

In this study, a reduced-scale model test (Kadente et al. 2021a; Kadente et al. 2021b; Kadente et al. 2023a; Kadente et al. 2023b) was designed to investigate the effect of the WDS on the water pressure of the initial and secondary linings, in which waterproof membranes, geotextiles, and blind pipes are considered. Based on the test observations, different than the previous solutions, an analytical solution is proposed that treats the initial and secondary lining separately and considers the effect of the entire WDS components to estimate the water pressure on each lining. The proposed analytical solution was then validated via model-test results. Parametric analysis and the WDS effect on water pressure were further investigated based on the proposed solution. The current research will be helpful to both practitioners and researchers involved in the design of composite linings and WDS of rock tunnels, and further provide theoretical support for the treatment of water leakage.

2 Model-Test Setup

2.1 Prototype Tunnel Condition

A prototype tunnel at the depth of 100 m and a groundwater level at the depth of 70 m was adopted, to investigate the effect of WDS on the water pressure distributions. The structural design and WDS details of the prototype tunnel are shown in Fig. 1.

As shown in Fig. 1, the composite lining comprises the initial lining, secondary lining, waterproof membranes, geotextile, and drainage pipes. To facilitate the research, the

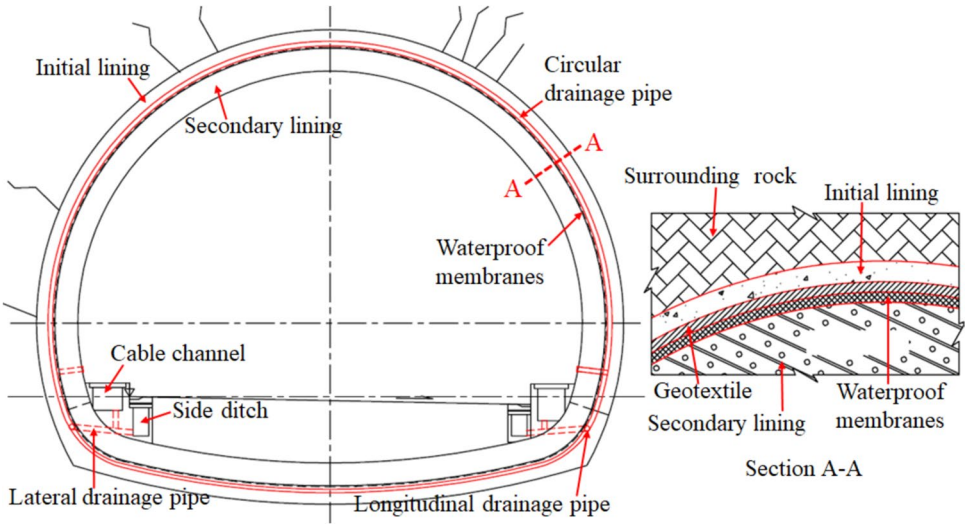

Fig. 1 Structure design and WDS detail of the prototype tunnel

Table 1 Parameters of the prototype tunnel

Parameters	Unit	Value
Outer radius of initial lining, r_2	m	5.8
Outer radius of secondary lining, r_1	m	5.5
Inner radius of secondary lining, r_0	m	5.1
Permeability coefficient of surrounding rock, k_r	m/s	2.0×10^{-5}
Thickness of geotextile, t	m	0.004
Permeability coefficient of geotextile, k_z	m/s	9.0×10^{-4}
Distance between two adjacent circular drainage pipes, L_1	m	10 ~ 20
Diameter of the circular drainage pipe, D	m	0.11

Table 2 Similarity ratio of the model test

Parameters of the similitude ratio	Definition	Relation
Length, C_L	$C_L=L_p/L_m$	$C_L=200$
Permeability, C_k	$C_k=k_p/k_m$	$C_k=\sqrt{200}$
Unit weight C_r	$C_\gamma=\gamma_p/\gamma_m$	$C_\gamma=1$
Time-scale, C_T	$C_T=T_p/T_m$	$C_T=C_L/C_k=\sqrt{200}$
Water pressure, C_p	$C_p=p_p/p_m$	$C_p=C_LC_\gamma=200$
Groundwater inflow, C_Q	$C_Q=Q_p/Q_m$	$C_Q=C_L^3/C_T=200^{\frac{5}{2}}$

actual section of the prototype tunnel was assumed equivalent to a circular tunnel for the experiment. The tunnel parameters are presented in Table 1.

2.2 Similitude Law of the Model Test

A reduced-scale model test was designed to simulate the seepage around the composite lining of the tunnel. The model test focuses on simulating the groundwater seepage field, and the Euler similarity criterion is applicable to the simulation of seepage field, pressure field, and water-flow pattern (Huang and Xu 2008). Thus, the Euler similarity criterion is adopted in the model test, where the Euler number is the ratio of hydrodynamic pressure to inertial force. Based on the similitude law (Baker et al. 1991; Tan et al. 2011; Liu et al. 2020b; Li and Liu 2021), the geometric (length) similarity ratio of the model test ($C_L=L_p/L_m$) was designed to be 200. The inner radius of the secondary lining of 5.1 m was represented by the model with an inner radius of 0.025 m. The outer radius of the secondary lining of 5.5 m was represented by the model with an outer radius of 0.0275 m. Here, L_p is a characteristic length in the prototype, and L_m is the corresponding length in the model. The similarity ratio of the permeability coefficient C_k is designed to be equal to $\sqrt{200}$, where the permeability coefficient of the surrounding rock was represented with a permeability of 2.0×10^{-5} m/s, as shown in Table 2.

In Table 2, L_p and L_m are the characteristic lengths; k_p and k_m are the permeability coefficients; γ_p and γ_m are the unit weights; T_p and T_m are the seepage times; p_p and p_m are the water pressures; and Q_p and Q_m are the amounts of groundwater inflow ("p" represents the prototype, and "m" represents the test model).

2.3 Model-Test Design

2.3.1 Selection of Materials

The permeability coefficient of the surrounding rock of the tunnel prototype is large, reaching the range of 10^{-5} m/s – 10^{-4} m/s in some sections with poor surrounding rock grade (Grade V sandstone) (Du et al. 2010). Therefore, based on the similitude law, a mixture of glass sand and kaolin, with a permeability coefficient of 2×10^{-5} m/s was

Fig. 2 Material of the surrounding rock (mixture consists glass sand and kaolin)

used as the material of the surrounding rock to facilitate groundwater seepage path observations during the tests, as shown in Fig. 2. The detailed properties of the remaining materials are listed in Table 3.

Based on the geometric similarity ratio, the thickness of geotextile material should be 0.02 mm, and the diameter of the circular drainage pipes should be 0.55 mm. In the model test, the geotextile thickness is set to be 2 mm (0.002 m) and the diameter of the circular drainage pipes is set to be 5.5 mm (0.0055 m) due to the limitation of the test material. According to Liu and Li (2021) and Li et al. (2021b), the increase of geotextile thickness will cause a decrease of water pressure value. Still, it will not affect the decreasing trend in water pressure, indicating that the seepage path and seepage gradient from initial lining to the circular pipes remain unchanged when the geotextile thickness increases, that is, the seepage mechanism of groundwater remain unchanged. Therefore, the thickness of the geotextile material in this test is enlarged. The groundwater flowing into the circular drainage pipes will continue to be discharged into the longitudinal drainage pipes, and the water discharge is not a seepage process (Bosseler et al. 2024). So, the enlargement of the diameter of the model pipes did not change the seepage path and seepage resistance gradient from the surrounding rock to the pipeline. The key to simulating the seepage field in model testing is to accurately simulate the groundwater seepage path and seepage gradient (Huang et al. 2023). Thus, enlarging the diameter of the drainage pipes and the thickness of the geotextile will not affect the seepage mechanism of the model test.

2.3.2 Test Instrumentation and Procedures

The model test apparatus comprised an experimental box, a water-supply device (including water tank, bracket, and pipes), and water pressure measurement tubes, as shown in Fig. 3. The size of the experimental box is 1.0 × 1.0 × 1.0 m; the box is made of a steel frame and plexiglass plate (Fig. 3b). The water pressure measurement tubes were made of vertical tubes and a wooden board, to fix the tubes (Fig. 3c).

All tests were performed per standardized test procedure (Kamel et al. 2024), to achieve the required level of repeatability. The preparation of each test is described below.

1) install the water supply device, experimental box, and pressure measurement tubes are installed as shown in Fig. 3;
2) the 35-cm thick surrounding rock material is paved evenly in the experimental box;
3) the measurement tubes are installed at the measuring points of composite lining model, as shown in Fig. 4.
4) The composite lining model was made of a circular drainage pipe, geotextile, waterproof membranes, and initial and secondary linings;
5) the composite lining in the experimental box is installed at the designed position (Fig. 4), and paved and the remaining surrounding rock material is filled evenly in the entire experimental box.
6) the water-supply pipes and pressure-measuring tubes are connected, and the water supply tank is filled with water.

Table 3 Materials of the experimental model

Model components	Materials	Permeability coefficient of the materials (m/s)
Surrounding rock	Mixture comprises glass sand and kaolin, and the mass ratio is 4:1	2.0×10^{-5}
Initial lining	Mixture comprises glass sand and kaolin, and the mass ratio is 1:1	2.4×10^{-6}
Secondary lining	Plexiglass tube with a diameter of 5 cm, on which holes are drilled to reserve the outlet of the circular drainage pipe	Secondary lining is impermeable
Circular drainage pipes	Springs wrapped in gauze, the spring diameter is 5.5 mm (0.0055 m), and the distance between two adjacent pipes is 10 cm	Groundwater inflow is discharged by drainage pipes
Geotextile	Geotextile with a specification of 400 kg/m^2, which thickness is 0.002 m	1.0×10^{-3}

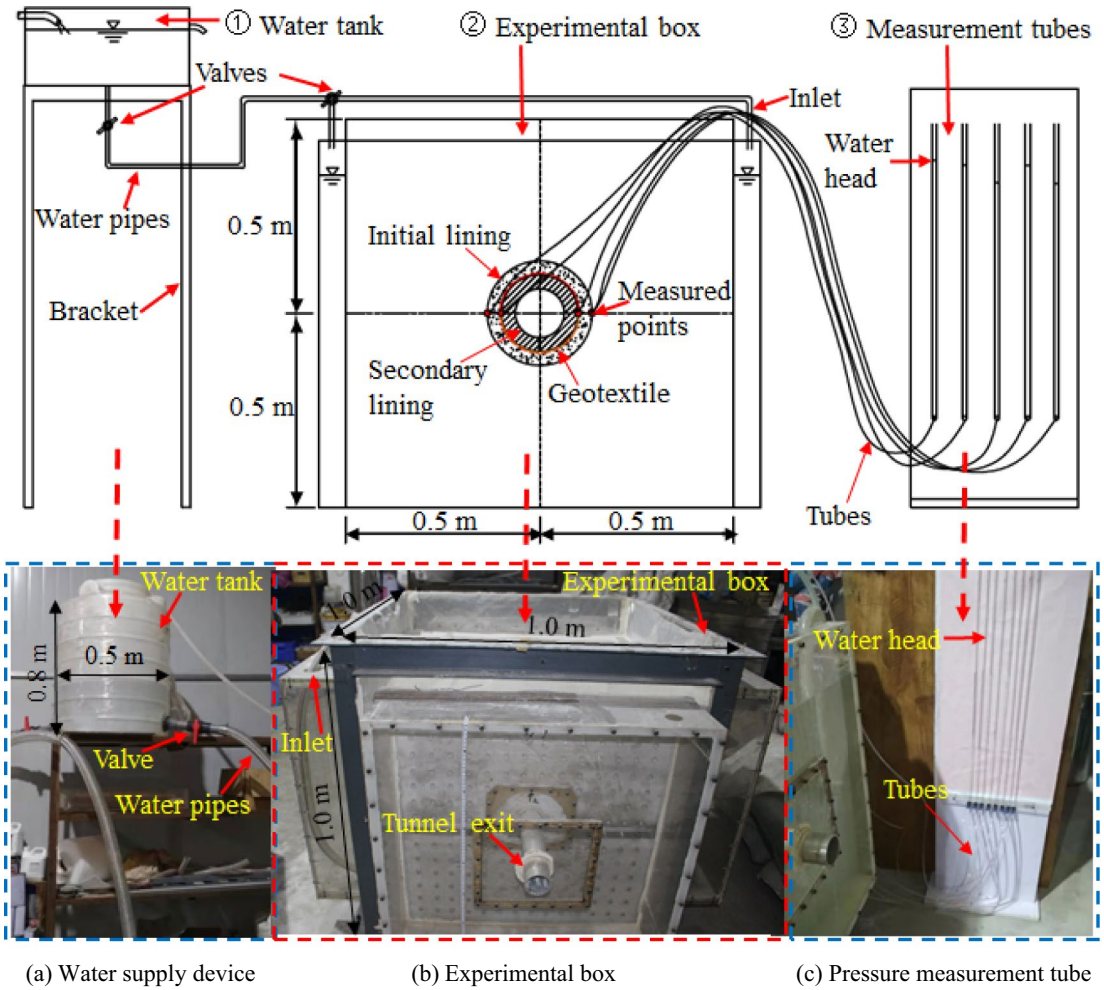

(a) Water supply device (b) Experimental box (c) Pressure measurement tube

Fig. 3 Configuration of the model test

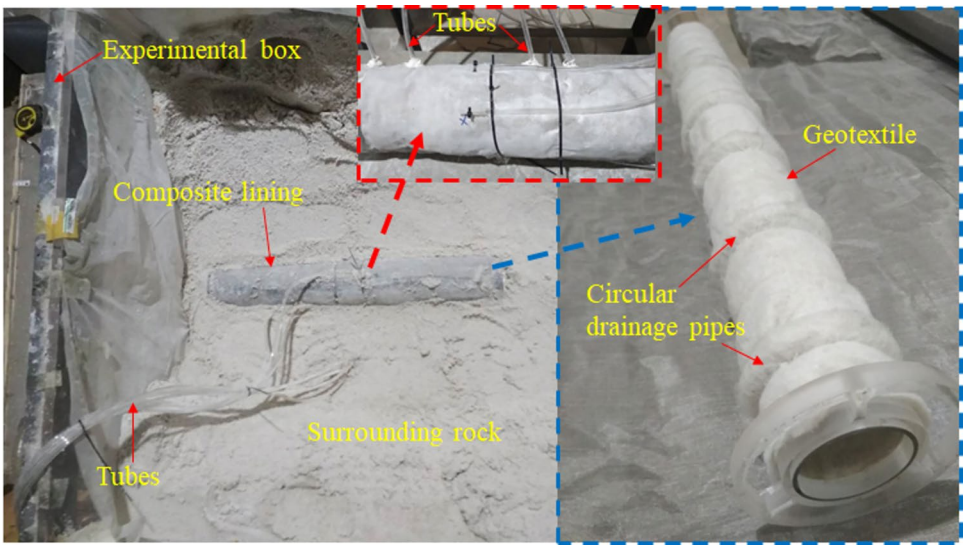

Fig. 4 Details of the model test

The experimental conditions range from 0.325 m–0.275 m water table, respectively 0.325 m, 0.315 m, 0.305 m, 0.295 m, 0.285 m, 0.275 m, a total of six test conditions. After the preparation, the test procedures were as follows. (1) the valve of the water supply device is turned on, to control the amount of water that is required to reach the water table of the experimental case; (2) when the water table reaches the predetermined test condition, it takes approximately 35 s to reach the steady state of seepage, in which the water head in all measurement tubes keeps unchanged. (3) the water head is recorded, acting on the composite lining, via the pressure-measuring device after the water table is stabilized in the experimental box and measuring device.

3 Analytical Solution

3.1 Water Drainage Seepage Model (WDSee)

Based on the test observations and practical engineering, a water drainage seepage (WDSee) model was established to derive the analytical solution of water pressure. The WDSee model, as the authors' previous research results, has been published (Liu and Li (2021)), as shown in Appendix A.

3.2 Derivation of the Analytical Solution

The governing equation of the steady-state groundwater flow in the surrounding rock can be expressed using the Laplace equation (Xiao et al. 2009; Liu 2017; Bear 1972).

$$\frac{\partial^2 h}{\partial r^2}+\frac{1}{r}\frac{\partial h}{\partial r}+\frac{1}{r^2}\frac{\partial^2 h}{\partial \theta^2}+\frac{\partial^2 h}{\partial z^2}=0 \tag{1}$$

where r is the radius, θ is the angle, z is the variable in the Z-axis, and h is the water head.

For deep tunnels with high-water table conditions, it can be assumed that the water head acting on the entire tunnel is equal (Zhang 2006; Wang et al. 2008). According to Bear (1972), Zhang (2006), and Wang et al. (2008), $\frac{\partial^2 h}{\partial z^2}=0$, $\frac{\partial^2 h}{\partial \theta^2}=0$, and thus, Eq. (1) can be simplified as

$$\frac{d^2 h}{dr^2}+\frac{1}{r}\frac{dh}{dr}=0 \tag{2}$$

After integrating Eq. (2), the following expression is obtained.

$$J=\frac{dh}{dr}=\frac{C}{r} \tag{3}$$

where J is the hydraulic gradient, and C is a constant.

According to Darcy's law and Eq. (3),

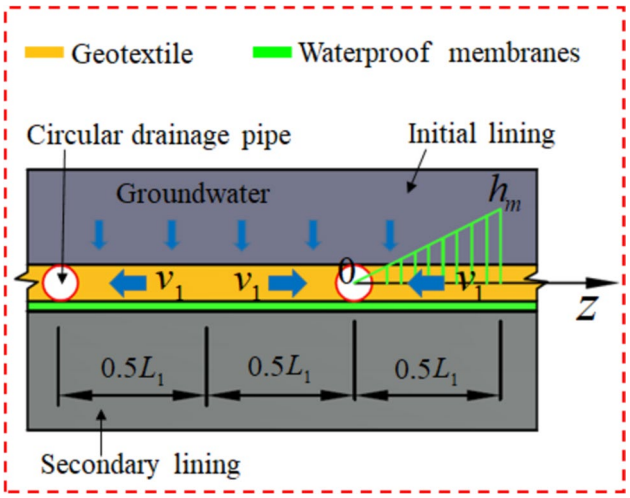

Fig. 5 Water-head distribution in the geotextile

$$J=\frac{v_0}{k}=\frac{Q}{2\pi rk},\ C=\frac{Q}{2\pi k} \tag{4}$$

where Q is the amount of groundwater inflow per meter, and v_0 is the seepage velocity.

According to Eq. (4), the following equation can be obtained for the surrounding rock considering $h\big|_{(r=r_3)}=H, h\big|_{(r=r_2)}=h_2$,

$$H-h_2=\frac{Q}{2\pi k_r}\ln\frac{r_3}{r_2} \tag{5}$$

The water-head difference between the initial and secondary linings can be obtained by considering $h\big|_{(r=r_2)}=h_2, h\big|_{(r=r_1)}=h(z)$ in the case of the initial lining.

$$h_2-h(z)=\frac{Q_{dz}}{2\pi k_1}\ln\frac{r_2}{r_1} \tag{6}$$

where Q_{dz} is the amount of groundwater flowing into the geotextile per element, and dz is the unit length in the longitudinal direction.

Based on assumption (3) and the results reported by Murillo et al. (2014) and Liu (2017), the governing equation of the geotextile can be simplified as

$$\frac{\partial^2 h}{\partial z^2}=0 \tag{7}$$

Assuming that the water head in the middle of the two drainage pipes is h_m, the boundary conditions of the geotextile can be expressed as $h\big|_{(z=0)}=0, h\big|_{(z=L_1/2)}=h_m$, as shown in Fig. 5.

The water-head distribution on the geotextile can be obtained by integrating Eq. (7).

$$h(z)=\frac{2zh_m}{L_1},\left(0<z<L_1/2\right) \tag{8}$$

where L_1 is the distance between two adjacent circular drainage pipes.

According to Eq. (6) and Eq. (8), the groundwater inflow per meter that flows into the geotextile from the initial lining Q can be obtained as

$$Q=\frac{\int_0^{\frac{L_1}{2}}Q_{dz}dz}{\frac{L_1}{2}}=\frac{2\pi k_1(h_2-\frac{h_m}{2})}{\ln\frac{r_2}{r_1}} \tag{9}$$

$$h_2-\frac{h_m}{2}=\frac{Q\ln\frac{r_2}{r_1}}{2\pi k_1} \tag{10}$$

The velocity of groundwater flowing into the circular drainage pipe from the geotextile can be obtained as

$$v_1=\frac{k_z(h_m-h\left|_{(r=r_0)}\right.)}{L_1/2}=\frac{2k_z(h_m-h\left|_{(r=r_0)}\right.)}{L_1} \tag{11}$$

In Fig. 5, the groundwater seeps into the circular drainage pipe at a constant rate of v_1. Accordingly, the groundwater inflow from the geotextile per meter into the circular drainage pipe can be expressed as

$$Q=\frac{\int_0^{2\pi}v_1tr_1d\theta}{L_1/2}=\frac{8\pi r_1k_zt(h_m-h_{|(r=r_0)})}{L_1^2} \tag{12}$$

$$h_m-h_{|(r=r_0)}=\frac{QL_1^2}{8\pi r_1k_zt} \tag{13}$$

where dθ is the unit circumferential length of the geotextile.

By combining Eqs. (5), (10), and (13), the water pressure on the initial lining, p_2, and maximal water pressure on the secondary lining, p_m, can be expressed as

$$p_2=\gamma h_2=\frac{\gamma H}{1+\frac{\ln\frac{r_3}{r_2}}{\beta}} \tag{14}$$

$$p_m=\gamma h_m=\frac{\gamma H}{\frac{1}{2}+\frac{4r_1tk_z}{L_1^2k_r}\ln\frac{r_3}{r_2}+\frac{4r_1tk_z}{L_1^2k_1}\ln\frac{r_2}{r_1}} \tag{15}$$

$$\beta=\frac{L_1^2k_r}{8r_1tk_z}+\frac{k_r}{k_1}\ln\frac{r_2}{r_1} \tag{16}$$

where β is defined as the drainage coefficient of the water pressure.

3.3 Comparison with the Existing Analytical Model

3.3.1 Zero Distance Between Two Adjacent Circular Drainage Pipes

The zero-distance condition is equivalent to a single-lining tunnel without a geotextile, waterproof membrane, or secondary lining. When subject to these conditions, Eqs. (14) and (15) can be simplified to

$$\lim_{L_1\to0}p_2=\lim_{L_1\to0}\frac{\gamma H}{1+\frac{\ln\frac{r_3}{r_2}}{\frac{L_1^2k_r}{8r_1tk_z}+\frac{k_r}{k_1}\ln\frac{r_2}{r_1}}}=\frac{\gamma H\ln\frac{r_2}{r_1}}{\ln\frac{r_2}{r_1}+\frac{k_1}{k_r}\ln\frac{r_3}{r_2}} \tag{17}$$

$$\lim_{L_1\to0}p_{aver}=\lim_{L_1\to0}\frac{p_m}{2}=\lim_{L_1\to0}\frac{\gamma H}{(\frac{1}{2}+\frac{4r_1tk_z}{L_1^2k_r}\ln\frac{r_3}{r_2}+\frac{4r_1tk_z}{L_1^2k_1}\ln\frac{r_2}{r_1})\times2}=0 \tag{18}$$

where $p_{\text{aver}}=p_{\text{m}}/2$ is the average water pressure on the secondary lining.

It can be found that Eq. (17) is identical to Wang's solution (Wang et al. 2008), where the average water pressure acting on the secondary lining, p_{aver}, was zero. Therefore, Wang's solution represents a particular case of the proposed analytical solution.

3.3.2 Infinite Distance Between Two Adjacent Circular Drainage Pipes

When the distance between two adjacent circular drainage pipes, L_1, approaches infinity, Eqs. (14) and (15) can be written as

$$\lim_{L_1\to\infty}p_2=\lim_{L_1\to\infty}\frac{\gamma H}{1+\frac{\ln\frac{r_3}{r_2}}{\frac{L_1^2k_r}{8r_1tk_z}+\frac{k_r}{k_1}\ln\frac{r_2}{r_1}}}=\gamma H \tag{19}$$

$$\lim_{L_1\to\infty}p_{aver}=\lim_{L_1\to\infty}\frac{p_m}{2}=\lim_{L_1\to\infty}\frac{\gamma H}{(\frac{1}{2}+\frac{4r_1tk_z}{L_1^2k_r}\ln\frac{r_3}{r_2}+\frac{4r_1tk_z}{L_1^2k_1}\ln\frac{r_2}{r_1})\times2}=\gamma H \tag{20}$$

In this situation, the entire water pressure, γH, is applied to the lining, where in the composite lining serves as an impermeable layer (Wang 2006).

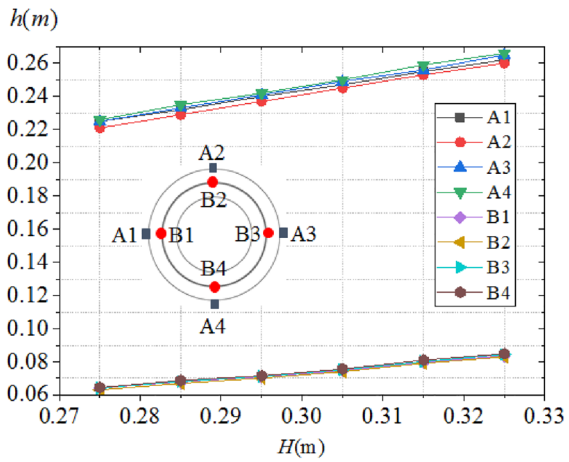

(a) Water pressure on the initial and secondary linings at four locations

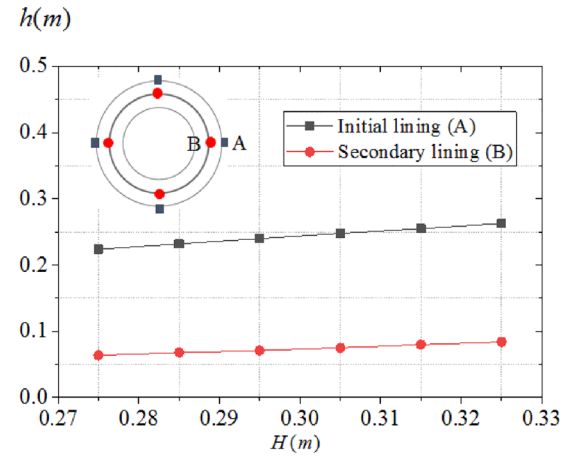

(b) Averages water pressure on the initial and secondary linings

Fig. 6 Water pressure on the initial and secondary linings for different water tables

4 Results

4.1 Model test results

The water pressure acting on the initial and secondary linings was measured at four locations (A1-A4, B1-B4), and the test results are shown in Table 5 of Appendix B. and the averages of the measurements are shown in Fig. 6.

As shown in Fig. 6, the water pressure on the initial lining increases from 0.224 to 0.263 m. The water pressure on the secondary lining increases from 0.064 to 0.084 m as the water table increases from 0.275 to 0.325 m. The water pressure acting on the initial lining was more significant than that on the secondary lining. For example, when the water table was 0.285 m, the water pressures on the initial and secondary linings were 0.232 and 0.068 m, respectively. Furthermore, the water pressure ratio on the initial lining to the water table, h_2/H, was approximately 81.5%, and the water pressure ratio on the secondary lining to the water head, h_m/H, was approximately 23.3% as the water table increased from 0.275 to 0.325 m. The model test readings showed that the ratios of h_2/H and h_m/H remained constant as the water table increased. This trend indicates that the water table has a weak effect on the distribution of the water pressure on the composite lining.

Figure 7 shows the results for the water pressure obtained using Liu's solution (Liu et al. 2013) and the model test, the water pressure date are listed in Table 6 of Appendix B. As shown in Fig. 7a, the water pressure on the initial lining of Liu's solution increases from 0.252 to 0.296 m, as the water table increases from 0.275 to 0.325 m. The difference between the model test and Liu's solution is approximately 13%, which is not apparent. However, the water pressure

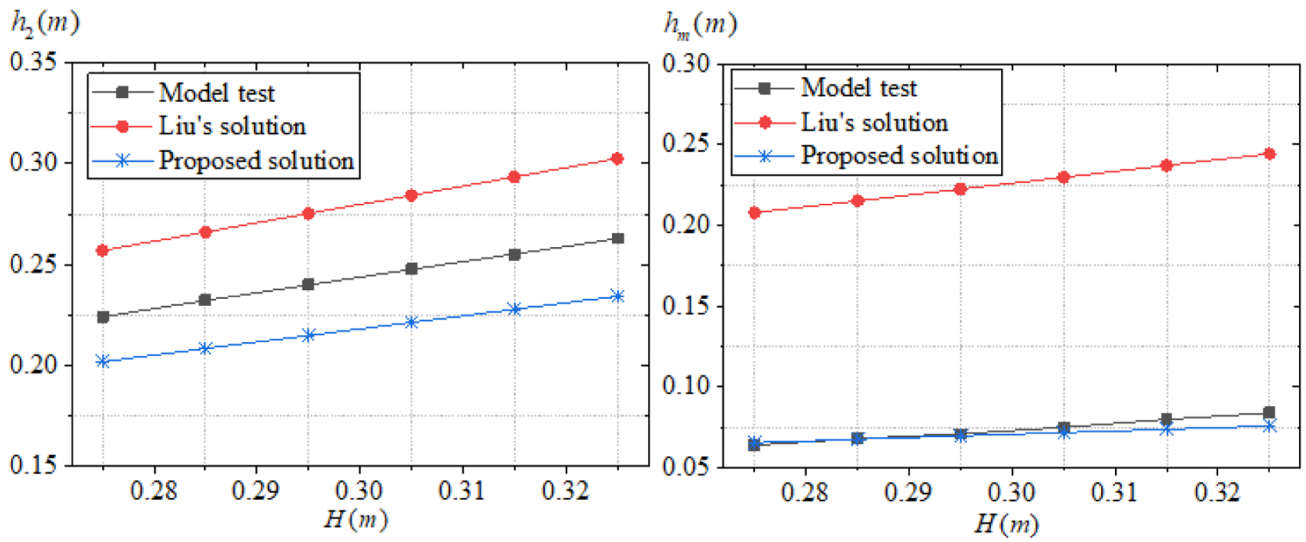

(a) Water pressure on the initial lining

(b) Water pressure on the secondary lining

Fig. 7 Comparison of water pressure between model test and analytical solutions

on the secondary lining of Liu's solution increases from 0.208 to 0.244 m, as the water table increases from 0.275 to 0.325 m, and the difference between the two methods is in the range of 191.0–225.0%, as shown in Fig. 7b. The difference between the model test (for the lined tunnel, considering all WDS components) and Liu's solution (for the lined tunnel, without considering the waterproof membranes, geotextile, and circular drainage pipes of the WDS) indicates that the effect of the WDS on the water pressure cannot be ignored. It can be concluded that the WDS reduces the water pressure on the secondary lining dramatically, while the effect on the initial lining is not evident when these experimental conditions are used.

4.2 Validation of the Analytical Solution

The proposed analytical solution of the water pressure on the composite lining was validated using the model test results. As shown in Fig. 7a, the water pressure on the initial lining of the proposed solution increases from 0.201 to 0.234 m. The model-test results increase from 0.224 to 0.263 m, as the water table increases from 0.275 to 0.325 m. The error between the proposed solution and model test results ranged from 9.9% to 10.9%. As shown in Fig. 7b, the water pressure on the secondary lining of the proposed solution increases from 0.065 to 0.076 m. The model-test results increase from 0.064 to 0.084 m, as the water table increases from 0.275 to 0.325 m. The errors between the proposed solution and model-test results ranged from –2.3% to 9.6%. Therefore, the proposed analytical solution is in good agreement with the model-test results.

4.3 Parametric Analysis

In this section, the permeability coefficient of the surrounding rock was set to 3×10^{-7} m/s. The remaining parameters are presented in Table 1. Two cases with different initial lining-permeability values (3×10^{-8} and 1×10^{-8} m/s) were considered. The water pressure ratio on the secondary lining to the initial lining, h_m/h_2, was used to investigate the water pressure distribution trend on the composite lining in the tunnel axis direction. The results of which are presented in the following sections.

4.3.1 Permeability Coefficient of Initial Lining

The relationship between the water pressure and the permeability coefficient of the initial lining, k_1, is shown in Fig. 8. The figure shows that an increase in the permeability coefficient of the initial lining, k_1, gradually reduces the water pressure acting on the initial lining to less than 10 m; meanwhile, the water pressure acting on the secondary lining increases from approximately 0.1 to 10 m. This tendency indicates that the water pressure acting on the initial lining decreases, while the water pressure acting on the secondary lining increases, as the permeability of the initial lining increases. The ideal condition in practical engineering is that both the water pressure on the initial lining and the secondary lining can be reduced. Thus, these findings will help design practitioners select a water pressure balance point between the two for designing the WDS.

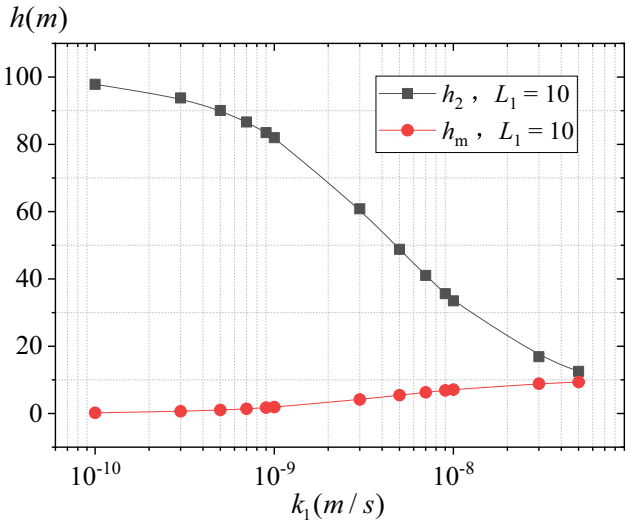

Fig. 8 Relationships between the water pressure and permeability coefficient of the initial lining

4.3.2 Distance Between two Adjacent Circular Drainage Pipes

The relationship between the water pressure and the distance between two adjacent circular drainage pipes, L_1, is shown in Fig. 9. The figure shows that the curve for the water pressure acting on the secondary lining is steeper than that for the initial lining as L_1 increases, thus demonstrating that the water pressure acting on the secondary lining is more sensitive to L_1 than that on the initial lining. When k_1 is 1×10^{-8} m/s, h_m/h_2 increases by approximately 55%, as L_1 increases from 2 to 20 m. This behavior demonstrates that the distance between two adjacent circular drainage pipes affects the water pressure distribution. A smaller distance leads to a higher reduction in the water pressure. Therefore, reducing the distance between two adjacent circular drainage pipes is a significant measure to reduce the water pressure on the secondary lining in practical engineering.

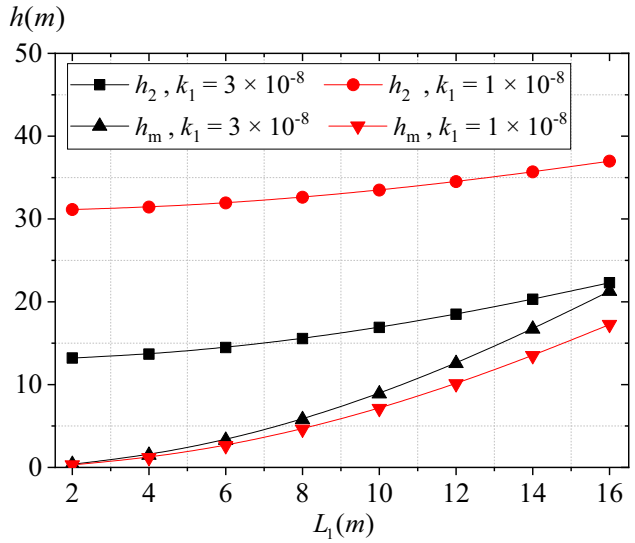

Fig. 9 Relationships between the water pressure and distance between two adjacent circular drainage pipes

4.3.3 Geotextile Hydraulic Conductivity

Figure 10 shows the relationship between the water pressure and the geotextile hydraulic conductivity, $k_z t$. Figure 10a shows that, when k_1 is 3×10^{-8} m/s, with $k_z t$ increasing from 2×10^{-6} to 1×10^{-5} m^2/s, the decrease in water pressures acting on the initial and secondary linings are 20% and 58%, respectively. When $k_z t$ was in the range of 5×10^{-6} – 1×10^{-5} m^2/s, each water pressure curve tended to be flat. This tendency suggests that $k_z t$ has a weak effect on the water pressure variation when $k_z t$ is higher than 5×10^{-6} m^2/s. As shown in Fig. 10b, when k_1 is 3×10^{-8} m/s, the ratio, h_m/h_2, decreases by 70% as $k_z t$ increases from 2×10^{-6} to 1×10^{-5} m^2/s, thus indicating that $k_z t$ has a significant effect on the water pressure distribution as $k_z t$ increases. Thus, increasing the geotextile hydraulic conductivity, such as laying a multi-layer geotextile, is an effective measure to reduce the water pressure on the secondary lining in practical engineering.

4.3.4 Permeability Coefficient Ratio of Surrounding Rock to Initial Lining

The relationship between the water pressure acting on the composite lining and k_r/k_1 is shown in Fig. 11. The results show that the water pressure acting on the initial lining, h_2, and secondary lining, h_m, increase more than ten times, as k_r/k_1 increases from 1 to 100, thus indicating that k_r/k_1 significantly affects the value of the water pressure. However, the ratio between the water pressure acting on the secondary and initial linings, h_m/h_2, remains constant as k_r/k_1 increases, implying that k_r/k_1 has a weak influence on the distribution of the water pressure on the composite lining.

4.4 The Effect of WDS

The permeability coefficient of the surrounding rock is a critical parameter for tunnel design in water-rich regions (Farhadian and Katibeh 2015). Therefore, it is used as the reference index to analyze the effects of the WDS on the water pressure. Figure 12 shows a comparison between the

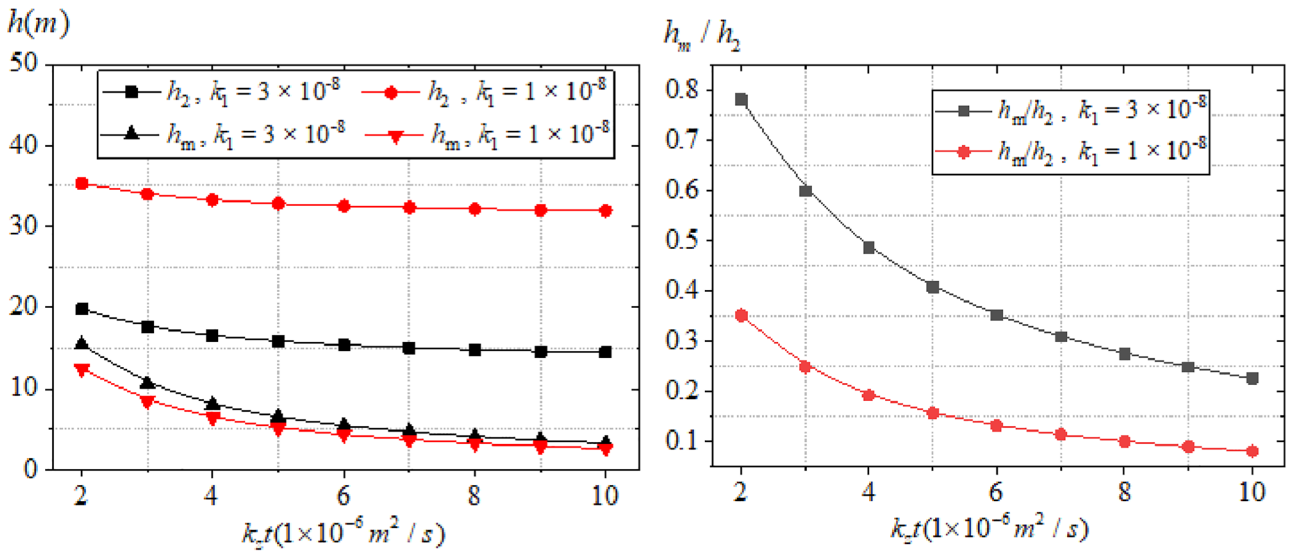

(a) Relationships between the water pressure and parameter $k_z t$ (b) Relationship between h_m/h_2 and $k_z t$

Fig. 10 Relationship between the water pressure and geotextile hydraulic conductivity

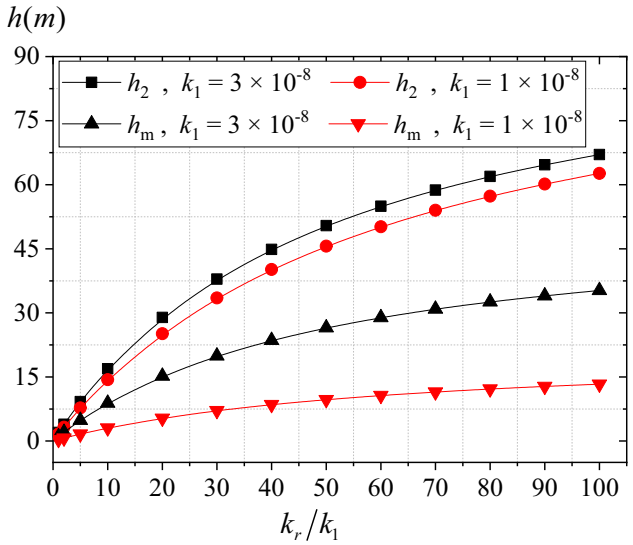

Fig. 11 Relationships of the water pressure and permeability coefficient ratio of the surrounding rock to initial lining, k_r/k_1

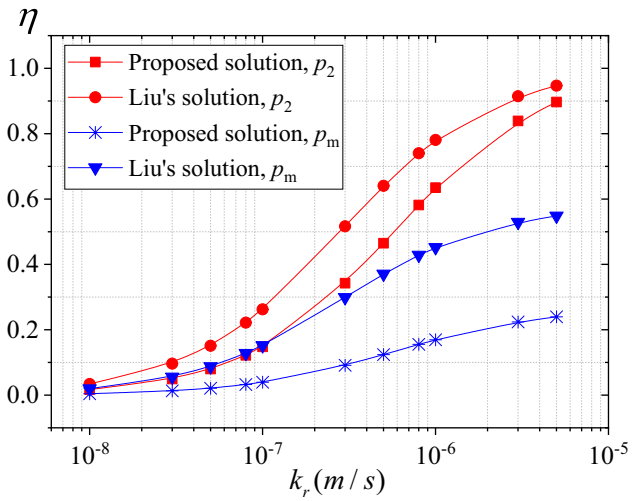

Fig. 12 Comparison of water pressure of the two analytical solutions

outcomes of Liu's solution (Liu et al. 2013) (lined tunnel without considering the waterproof membranes, geotextile, and circular drainage pipes) and the proposed analytical solution (lined tunnel considering all WDS components) for the water pressure acting on the initial lining, p_2, and secondary lining, p_m. The results of the water pressure are expressed as ratio $\eta = p/rH$ in Fig. 12; here, the initial lining permeability of the results is 1×10^{-8} m/s.

As shown in Fig. 12, all curves exhibit an "S"-shape behavior, where the slope is flat at first, which is followed by a steep rise, and then, gradually becomes flat. The initial lining ratio curve of the proposed solution, η, increased from 0.017 to 0.897, as the surrounding rock permeability increased from 1×10^{-8} to 5×10^{-6} m/s.

5 Discussion

5.1 Model Test

There is a 13% difference in water pressure on the initial lining between the model test and Liu's solution. As shown in Fig. 7, the difference ranges from 191.0 to 225.0% for the water pressure on the secondary lining. Liu's model assumes that the groundwater infiltrates the secondary lining into the tunnel instead of being discharged into the tunnel through drainage pipes. This assumption will overestimate the seepage resistance of groundwater entering the tunnel, that is, the waterproof performance of the secondary lining in Liu's model is much greater than that of the geotextile and drainage system in the actual tunnel. Therefore, the smaller permeability of the secondary lining leads to an overestimation of water pressure. Meanwhile, a smaller permeability coefficient of the secondary lining will cause a significant increase in the water pressure loaded on the secondary lining.

5.2 Inclusion of WDS

The analysis results in Fig. 8 indicate that the initial lining-permeability coefficient notably influences the water pressure. When the permeability coefficient increases, water pressure on the secondary and initial lining exhibits two distinct trends, that is, the water pressure of the secondary lining increases while the water pressure of the initial lining decreases. The reason for this trend is that the increase of the permeability coefficient of the initial lining reduces the waterproof effect of the initial lining and the water-head gradient acting on the initial lining. This decreases the water pressure acting on the initial lining and increases the internal pressure acting on the secondary lining.

The analysis results in Fig. 12 indicates that the surrounding rock permeability coefficient has a notable influence on the water pressure. Furthermore, when the rock permeability is higher than 5×10^{-7} m/s, the difference ($\delta = (p_{\text{proposed}} - p_{\text{Liu}})/p_{\text{Liu}} \times 100\%$) of the water pressure on the initial lining remains in the range of −5.0%–−25.8%, while the corresponding difference of the secondary lining in the range of −54.1%–−64.1%, as shown in Table 4. When the rock permeability is less than 5×10^{-7} m/s, the water pressure differences on the initial and secondary linings are in the ranges of −25.8%–−47.4% and −64.1%–−74.6%, respectively. The trends indicate a significant effect of the WDS on the water pressure of the secondary lining.

The proposed solution used for the prediction of the water pressure was derived based on the assumption that the tunnel

Table 4 The water-pressure difference of the two analytical solutions

Surrounding rock permeability coefficient, k_r(m/s)	Comparison of initial lining			comparison of secondary lining		
	Proposed solution, $\eta_2 = p_2/rH$	Liu's solution, $\eta_2 = p_2/rH$	The difference,δ	Proposed solution, $\eta_m = p_m/rH$	Liu's solution, $\eta_m = p_m/rH$	The difference,δ
5×10^{-6}	0.897	0.944	−5.0%	0.240	0.522	−54.1%
3×10^{-6}	0.839	0.910	−7.8%	0.224	0.503	−55.4%
1×10^{-6}	0.635	0.770	−17.6%	0.170	0.426	−60.2%
8×10^{-7}	0.582	0.729	−20.2%	0.156	0.403	−61.4%
5×10^{-7}	0.465	0.627	−25.8%	0.124	0.347	−64.1%
3×10^{-7}	0.343	0.502	−31.7%	0.092	0.278	−67.0%
1×10^{-7}	0.148	0.251	−41.1%	0.040	0.139	−71.5%
8×10^{-8}	0.122	0.212	−42.3%	0.033	0.117	−72.1%
5×10^{-8}	0.080	0.144	−44.4%	0.021	0.080	−73.1%
3×10^{-8}	0.050	0.092	−45.8%	0.013	0.051	−73.8%
1×10^{-8}	0.017	0.032	−47.4%	0.005	0.018	−74.6%

cross-section was circular. Although this is often untrue in practical engineering, an equivalent circular shape may be used in most cases. In addition, the surrounding rock is assumed to be a continuous porous medium, considering that the tunnel size is larger than the representative elementary volume (Li 2018). In practice, the fractured rock mass has a discontinuous nature (Katende 2022; Zhang et al. 2024); however, the effect of the discontinuities is negligible in densely distributed fissures (Wang et al. 2008; Fatehi et al. 2024). Therefore, the proposed analytical solution can also be applied to tunnels in rock masses with densely distributed fractures. When the tunnel is a shallow tunnel, significant errors may occur. Therefore, the proposed solution can be used for deep rock tunnels.

5.3 Application Discussion

In practical engineering, tunnel engineers need to calculate the water pressure acting on the linings to design the lining structure when designing the support system of a tunnel. This proposed solution can predict the water pressure on the linings considering the entire WDS. In addition, through this study, we found that the WDS will significantly affect the magnitude of the water pressure acting on the linings. Practitioners can use the proposed analytical solution to optimize the layout of the WDS to reduce the water pressure load on the lining. For example, laying multi-layer geotextile and reducing the distance between two adjacent circular drainage pipes are significant measures to reduce the water pressure on the secondary lining in practical engineering. Thus, the current research will be helpful to both practitioners and researchers involved in the design of composite linings and WDS of rock tunnels, and further provide theoretical support for the treatment of tunnel groundwater leakage. In the following research, we will apply the proposed solution to practical engineering, and further explore systematic optimization methods for WDS based on the proposed solution.

6 Conclusions

A reduced-scale model test was designed to investigate the effect of WDS on water pressure, and to explore the water pressure distribution on a composite lining. Based on the test results, an analytical solution was derived for estimating the water pressure acting on the composite lining (including the initial and secondary linings), which fully considered the WDS effect. The proposed analytical solution was in good agreement with the model-test results. Consequently, the following conclusions were drawn:

1) The WDS dramatically reduced the water pressure on the secondary lining, while the effect of the WDS on the water pressure of the initial lining was not significant. As the initial lining permeability increased, the water pressure acting on the initial lining decreased, and the water pressure acting on the secondary lining increased. When the permeability coefficient of the surrounding rock was in the range of 1×10^{-8} to 5×10^{-6} m/s, the difference in water pressure on the secondary lining between the proposed solution and Liu's solution was greater than 54.1%. Therefore, the WDS effect on the water pressure of the secondary lining cannot be ignored in these conditions.
2) The proposed analytical solution can be used to predict the water pressure acting on the initial and secondary linings, when the tunnel is at a large depth with a high-water table. The proposed analytical solution can be reduced to Wang's solution (Wang et al. 2008) for an infinitesimal distance between two adjacent circular

Fig. 13 WDSee model

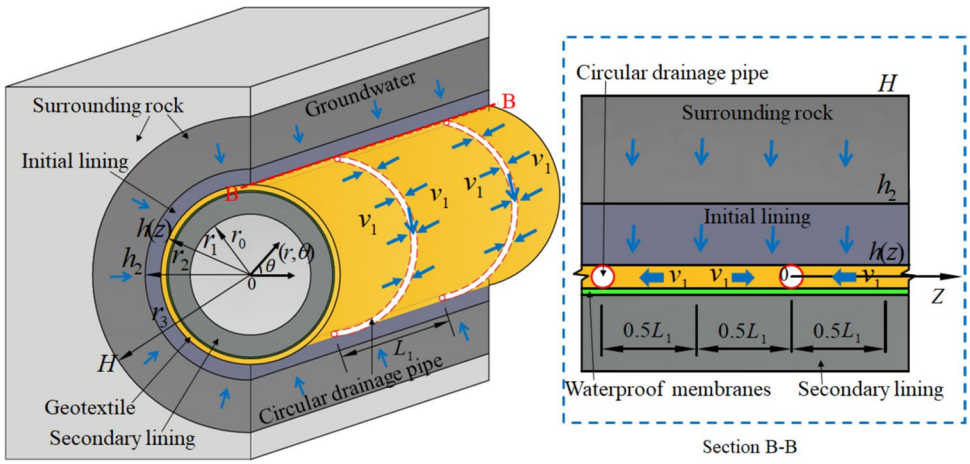

drainage pipes (or a single-layer lining). In this case, the entire water pressure is applied to the lining without circular drainage pipes, and the composite lining serves as an impermeable layer.

3) The water–pressure distribution on the composite lining was affected by the distance between two adjacent circular drainage pipes, permeability coefficients and geotextile thickness, and the initial lining permeability. These findings can provide theoretical base for tunnel design with controlled drainage. For example, laying multilayer geotextile and reducing the distance between two adjacent circular drainage pipes are significant measures to reduce the water pressure on the secondary lining in practical engineering.

This study has several limitations. First, the analytical solution only considered Darcy flow, but non-Darcy flow may occur under high hydraulic gradients (Zhang et al. 2019). Second, the solution is only applicable to circular tunnels. Finally, the analytical solution cannot explicitly characterize the influence of fracture flow (Shahbazi et al. 2021). In future work, we will focus on addressing these three limitations and exploring systematic optimization methods for WDS.

Appendix A

This appendix explains the design and assumptions of the water drainage seepage (WDSee) model in Sect. 3.1.

The configuration of the WDSee model is shown in Fig. 13. In the model, the groundwater flows from the surrounding rock into the initial lining, which is followed by the geotextile, and finally, reaches the circular drainage pipes. Such groundwater seepage processes obey Darcy's law (Murillo et al. 2014; Ying et al. 2016; Farhadian and Katibeh 2017). When the groundwater flows into the circular drainage pipes, it is discharged through the longitudinal and lateral drainage pipes. Because the water discharge is not a seepage process, the longitudinal and lateral drainage pipes were excluded from the proposed model.

As shown in Fig. 13, parameters r_0 and r_1 are the inner and outer radii of the secondary linings, respectively; r_2 is the outer radius of the initial lining; and r_3 is the radius of the drainage-affected zone. Moreover, h_2 is the water head around the initial lining, and h(z) is the water head at the geotextile. H is the water head around the drainage-affected zone in the surrounding rock. In addition, k_1 is the permeability coefficient of the initial lining, and k_r is the permeability coefficient of the surrounding rock. The distance between two adjacent circular drainage pipes was defined as L_1. The thickness of the geotextile is expressed as t, and its permeability coefficient is denoted as k_z.

The basic assumptions of the WDSee model are listed as follows.

1) Groundwater seepage follows the law of conservation of mass (Wu and Xue 2009; Hassani et al. 2018), meaning that the amount of groundwater flowing into the surrounding rock, initial lining, and geotextile is equal. Groundwater is finally discharged through the circular drainage pipes (Wang 2006).
2) The aquifer is homogeneous and isotropic (Kolymbas and Wagner 2007), and the water table is assumed to be high and steady in the horizontal direction (Park et al. 2008; Tan et al. 2017). The seepage in the surrounding rock, initial lining, and geotextile follows Darcy's law (Murillo et al. 2014; Ying et al. 2016; Farhadian and Katibeh 2017).
3) The groundwater flows along the radial direction in the surrounding rock and initial lining (Zhang 2006; Wang et al. 2008; Li et al. 2018), and penetrates uniformly into the circular drainage pipes from the geotextile at a constant rate (Wang et al. 2004), as shown in Fig. 13.

Table 5 The model test data used in this paper

Water table H (m)	Water pressure on initial lining h_2 (m)					Water pressure on secondary lining h_m (m)				
	A1	A2	A3	A4	Average value	B1	B2	B3	B4	Average value
0.325	0.262	0.26	0.265	0.266	0.263	0.084	0.083	0.085	0.085	0.084
0.315	0.255	0.253	0.256	0.259	0.256	0.080	0.079	0.080	0.081	0.080
0.305	0.247	0.245	0.249	0.25	0.248	0.075	0.074	0.075	0.076	0.075
0.295	0.24	0.237	0.241	0.242	0.240	0.071	0.070	0.071	0.072	0.071
0.285	0.232	0.229	0.233	0.235	0.232	0.068	0.067	0.068	0.069	0.068
0.275	0.225	0.221	0.225	0.226	0.224	0.064	0.063	0.064	0.065	0.064

Table 6 The water pressure data of Liu's solution and the proposed solution

Water table H(cm)	Water pressure on initial lining h_2 (m)			Water pressure on secondary lining h_m (m)		
	Proposed solution	Liu's solution	Model test	Proposed solution	Liu's solution	Model test
0.325	0.234	0.296	0.263	0.076	0.244	0.084
0.315	0.228	0.286	0.256	0.074	0.237	0.080
0.305	0.221	0.278	0.248	0.071	0.230	0.075
0.295	0.215	0.269	0.240	0.067	0.223	0.071
0.285	0.208	0.260	0.232	0.068	0.215	0.068
0.275	0.201	0.252	0.224	0.065	0.208	0.064

The groundwater flows along the tunnel axis direction within the geotextile (Murillo et al. 2014; Wang 2006; Liu 2017), as shown in section B-B in Fig. 13.

According to the above assumptions, the boundary conditions of the WDSee model can be expressed as presented below:

1. the boundary condition at the radius of the affected drainage zone is $h\big|_{(r=r_3)} = H$;
2. the boundary condition at the outer radius of the initial lining is $h\big|_{(r=r_2)} = h_2$;
3. the boundary condition at the outer radius of the secondary lining is $h\big|_{(r=r_1)} = h(z)$;
4. the boundary condition at the inner radius of the secondary lining is $h\big|_{(r=r_0)} = 0$.

Appendix B

This appendix lists all the test data used in this paper, as shown in Tables 5 and 6. The sections that use the data include Sects. 4.1, 4.2, and 5.1.

Acknowledgements The research was supported by the National Natural Science Foundation of China (Grant No. 41877246), Department of Transport of Yunnan Province (Grant No. [2019]36), and sponsored by the Anhui Transportation Holding Group Co. Ltd. (JKKJ-2020-10). The authors greatly appreciate the support provided.

Author contributions Jinghui Liu: Model test, Data analysis, Derivation, Validation, Writing original draft. Cagri Gokdemir: Data analysis, Writing-review & editing. Xiaojun Li: Conceptualization, Funding acquisition, Methodology. Yue Xi: Model test, Writing-review.

Funding National Natural Science Foundation of China, 41877246, Xiaojun Li, Department of Transport of Yunnan Province,No. [2019]36, Xiaojun Li

Data availability The data that support the findings of this study are available from the corresponding author upon reasonable request.

Declarations

Conflict of interest The authors declare that they have no conflict of interest.

References

Bagnoli P, Bonfanti M, Della Vecchia G, Lualdi M, Sgambi L (2015) A method to estimate concrete hydraulic conductivity of underground tunnel to assess lining degradation. Tunn Undergr Space Technol 50:415–423. https://doi.org/10.1016/j.tust.2015.08.008

Baker WE, Westine PS, Dodge FT (1991) Similarity Methods in Engineering Dynamics—Theory and Practice of Scale Modeling. Elsevier Science, Netherlands

Bear J (1972) Dynamics of Fluids in Porous Media. American Elsevier Publishing Company, New York

Bian K, Xiao M, Chen JT (2009) Study on coupled seepage and stress fields in the concrete lining of the underground pipe with high water pressure. Tunn Undergr Space Technol 24:287–295. https://doi.org/10.1016/j.tust.2008.10.003

Bosseler B, Homann D, Brüggemann T, Naismith I, Rubinato M (2024) Quality assessment of CIPP lining in sewers: Crucial knowledge acquired by IKT and research gaps identified in Germany. Tunn Undergr Space Technol 143:105425

Chen K, Liu N (2023) Study on drainage mode and anti-clogging performance of new waterproofing and drainage system in a tunne1. Sci Rep 13:5354. https://doi.org/10.1038/s41598-023-32590-9

Ding H, Jiang SP, Li Y (2007) Study on waterproof and drainage techniques of tunnels based on controlling drainage. Chin J Geotech Eng 29(9):1398–1403

Du X, Zeng YW, Tang DY (2010) Research on permeability coefficient of rock mass based on underwater pumping test and its application. Chin J Rock Mech Eng 29(S2):3542–3548

Du CW, Wamg MS, Tan ZS (2011) Analytic solution for seepage filed of subsea tunnel and its application. Chin J Rock Mech Eng 30(S2):3567–3573

Fan HY, Li LP, Chen GQ et al (2023) Analysis method of the water inrush and collapse in jointed rock mass tunnels: a case study. Eng Anal Bound Elem 146:838–850. https://doi.org/10.1016/j.enganabound.2022.11.030

Fang Y, Guo J, Grasmick J, Mooney M (2016) The effect of external water pressure on the liner behavior of large cross-section tunnels. Tunn Undergr Space Technol 60:80–95. https://doi.org/10.1016/j.tust.2016.07.009

Farhadian H, Katibeh H (2015) Effect of model dimension in numerical simulation on assessment of water inflow to tunnel in discontinues rock World Academy of Science, Engineering and Technology. Int J Civil Environ Eng 9(4):257–260

Farhadian H, Katibeh H (2017) New empirical model to evaluate groundwater flow into circular tunnel using multiple regression analysis. Int J Min Sci Technol 27(3):415–421. https://doi.org/10.1016/j.ijmst.2017.03.005

Farhadian H, Nikvar-Hassani A (2018) Water flow into tunnels in discontinuous rock: a short critical review of the analytical solution of the art. Bull Eng Geol Env 78(5):3833–3849

Fatehi H, Ong DE, Yu J, Chang I (2024) Sustainable soil treatment: Investigating the efficacy of carrageenan biopolymer on the geotechnical properties of soil. Constr Build Mater 411:134627

Gao XQ, Qiu WG (2004) Research present situation and advance of calculation methods of external water pressure for tunnel lining. Railw Stand Des 48(12):84–87

Golian M, Abolghasemi M, Hosseini A, Abbasi M (2021) Restoring groundwater levels after tunneling: a numerical simulation approach to tunnel sealing decision-making. Hydrogeol J 29:1611–1628. https://doi.org/10.1007/s10040-021-02315-1

Hassani NA, Farhadianb H, Katibeh H (2018) A comparative study on evaluation of steady-state groundwater inflow into a circular shallow tunnel. Tunn Undergr Space Technol 73:15–25. https://doi.org/10.1016/j.tust.2017.11.019

He BG, Zhang ZQ, Fu SJ, Liu YJ (2015) An analytical solution of water loading on tunnel supporting system with drainage of blind tube and isolation effect of waterproof membranes. Chin J Rock Mech Eng 34(Suppl2):3936–3947

Huang LC, Xu GX (2008) Hydraulic and River Model Tests. Yellow River Conservancy Press, Zhengzhou, China

Huang M, Yang Z, Song Y, Zhang Z (2023) Large-scale model test study on the water pressure resistance of construction joints of karst tunnel linings. Front Struct Civ Eng 17(8):1249–1263

Huangfu M, Wang MS, Tan ZS, Wang XY (2010) Analytical solutions for steady seepage into an underwater circular tunnel. Tunn Undergr Space Technol 25:391–396. https://doi.org/10.1016/j.tust.2010.02.002

Jansson R, Boström L (2010) The influence of pressure in the pore system on fire spalling of concrete. Fire Technol 46:217–230. https://doi.org/10.1007/s10694-009-0093-9

Kamel E, Habibi S, Memari AM (2024) State of the practice review of moisture management in residential buildings through sensors. Structures, vol 59. Elsevier, p 105698

Katende A, O'Connell L, Rich A et al (2021a) A comprehensive review of proppant embedment in shale reservoirs: Experimentation, modeling and future prospects. J Nat Gas Sci Eng 95:104143. https://doi.org/10.1016/j.jngse.2021.104143

Katende A, Rutqvist J, Benge M et al (2021b) Convergence of micro-geochemistry and micro-geomechanics towards understanding proppant shale rock interaction: a Caney shale case study in southern Oklahoma, USA. J Nat Gas Sci Eng 96:104296. https://doi.org/10.1016/j.jngse.2021.104296

Katende A, Allen C, Rutqvist J et al (2023a) Experimental and numerical investigation of proppant embedment and conductivity reduction within a fracture in the Caney Shale, Southern Oklahoma, USA. Fuel 341:127571. https://doi.org/10.1016/j.fuel.2023.127571

Katende A, Rutqvist J, Massion C et al (2023b) Experimental flow-through a single fracture with monolayer proppant at reservoir conditions: a case study on Caney Shale, Southwest Oklahoma, USA. Energy 273:127181. https://doi.org/10.1016/j.energy.2023.127181

Katende A (2022) The Impact of rock lithology and microstructural properties on proppant embedment and fracture conductivity: A case study of the Caney Shale, Southern Oklahoma, USA. Doctoral dissertation, Oklahoma State University.

Kolymbas D, Wagner P (2007) Groundwater ingress to tunnels the exact analytical solution. Tunn Undergr Space Technol 22:23–27

Li W (2018) Characteristic scales for permeable property of fractured rock masses in typical flow configurations and engineering applications. Shandong University, Jinan

Li XJ, Liu JH (2021) Effect of waterproof and drainage system on seepage properties of composite lining and its characterization method. J Tongji Univ 49(7):995–1003

Li P, Wang F, Long Y, Xu Z (2018) Investigation of steady water inflow into a subsea grouted tunnel. Tunn Undergr Space Technol 80:92–102

Li SC, Gao CL, Zhou ZQ et al (2019) Analysis on the precursor of water inrush in karst tunnels: a true triaxial model test study. Rock Mech Rock Eng 52:373–384. https://doi.org/10.1007/s00603-018-1582-2

Li Z, Li ZQ, Cai RY, Hua Y, Wang L, Gu DM (2021b) Refined model analysis of basement rock degradation mechanism of heavy-haul railway tunnel. Undergr Space 6(3):342–352

Li LP, Hu J, Li SC et al (2021a) Development of a novel triaxial rock testing method based on biaxial test apparatus and its application. Rock Mech Rock Eng 54(3):1597–1607. https://doi.org/10.1007/s00603-020-02329-3

Liu K (2017) Study on external water pressure and force characteristics of tunnel lining with partial blocked drainage system. Chongqing University, Chongqing

Liu JH, Li XJ (2021) Analytical solution for estimating groundwater inflow into lined tunnels considering waterproofing and drainage systems. Bull Eng Geol Env 80:6827–6839. https://doi.org/10.1007/s10064-021-02378-0

Liu L, Wang X, Jia Z, Duan Q, Wang Y (2013) Method to determine reduction factor of water pressure acting on tunnel linings using water-rock independent calculation methodology. Chin J Geotech Eng 35(3):495–500

Liu Y, Feng Y, Xu M, Zhang Y, Zhu H (2019) Effect of an incremental change in external water pressure on tunnel lining: a case study from the tongxi karst tunnel. Nat Hazards 98(2):343–377

Liu MZ, Zhang H, Yang J, Zheng W, You S (2020a) Application of distortion theory to tunnel physical modeling. Build Environ 177:0360–1323. https://doi.org/10.1016/j.buildenv.2020.106845

Liu Q, Zhao Z, Nie W et al (2020) An analytical investigation on the estimation of water inflow into a circular tunnel based on-site data. Rock Mech Rock Eng 53:3835–3844. https://doi.org/10.1007/s00603-020-02114-2

Liu X, Wang DC, Zhang Y, Jiang AN, Fang Q, Zhang R (2023) Analytical solutions on non-Darcy seepage of grouted and lined subsea

tunnels under dynamic water levels. Ocean Eng 267:113276. https://doi.org/10.1016/j.oceaneng.2022.113276
Maleki MR (2018) Groundwater Seepage Rate (GSR); a new method for prediction of groundwater inflow into jointed rock tunnels. Tunn Undergr Space Technol 71:505–517
Murillo CA, Shin JH, Kim KH, Colmenares JE (2014) Performance tests of geotextile permeability for tunnel drainage systems. KSCE J Civ Eng 18(3):827–830
Nikvar-Hassani A, Katibeh H, Farhadian H (2016) Numerical analysis of steady-state groundwater inflow into Tabriz line 2 metro tunnel, northwestern Iran, with special consideration of model dimensions. Bull Eng Geol Env 75(4):1617–1627
Park KH, Lee JG, Owatsiriwong A (2008) Seepage force in a drained circular tunnel: an analytical approach. Can Geotech J 45(3):432–436
Parker ST, Lorenzetti DM, Sohn MD (2014) Implementing state-space methods for multizone contaminant transport. Build Environ 71:131–139. https://doi.org/10.1016/j.buildenv.2013.09.021
Ponlawich A, Jeong JH, Kim CY, Park KH (2009) Effect of drainage conditions on pore water pressure distributions and lining stresses in drained tunnels. Tunn Undergr Space Technol 24:376–389
Preisig G, Dematteis A, Torri R et al (2014) Modelling discharge rates and ground settlement induced by tunnel excavation. Rock Mech Rock Eng 47:869–884. https://doi.org/10.1007/s00603-012-0357-4
Shahbazi A, Chesnaux R, Saeidi A (2021) A new combined analytical-numerical method for evaluating the inflow rate into a tunnel excavated in a fractured rock mass. Eng Geol 283:106003. https://doi.org/10.1016/j.enggeo.2021.106003
Shin JH, Shin YS, Kim SH, Shin HS (2007) Evaluation of residual pore water pressures on linings for undersea tunnels. Chin J Rock Mech Eng 26(Supp. 2):3682–3685
Shin HS, Youn DJ, Chae SE, Shin JH (2009) Effective control of pore water pressures on tunnel linings using pin-hole drain method. Tunn Undergr Space Technol 24:555–561
Tan ZS, Zeng C, Li J, Du C, Zhang P (2011) Model test investigation on the mechanical characteristics of support structure of subsea tunnels. Civil Eng J 44(11):99–105
Tan Y, Smith JV, Li CQ, Currell M, Wu Y (2017) Predicting external water pressure and cracking of a tunnel lining by measuring water inflow rate. Tunn Undergr Space Technol 71:115–125. https://doi.org/10.1016/j.tust.2017.08.015
Tang Y, Chan DH, Zhu DZ (2018) Analytical solution for steady-state groundwater inflow into a circular tunnel in anisotropic soils. J Eng Mech 144(9):1–8
Teng Z, Liu Y, Mei S, Zhou Y, He G, Li Y et al (2023) FEM analysis of a new three-way drainage and pressure reduction system for road tunnels. Sci Rep. https://doi.org/10.1038/s41598-023-37417-1
The Ministry of Water Resources of the People's Republic of China (2016) Specification for hydraulic tunnel. SL279–2016. China Water & Power Press, Beijing.
Wang YC (2006) Tunnel engineering. China Communications Press, Beijing
Wang JY (2008) Problems on external water pressure on tunnel lining. Railw Constr Technol 2:1–6
Wang XY, Wang MS, Zhang M (2004) A simple method to calculate tunnel discharge and external water pressure on lining. J Northern Jiaotong Univ 28(1):8–10
Wang XY, Tan ZS, Wang MS, Zhang M, Huangfu M (2008) Theoretical and experimental study of external water pressure on tunnel lining in controlled drainage under high water level. Tunn Undergr Space Technol 23:552–560. https://doi.org/10.1016/j.tust.2007.10.004
Wei ZL, Wang DF, Xu HD, Sun HY (2020) Clarifying the effectiveness of drainage tunnels in landslide controls based on high-frequency in-site monitoring. Bull Eng Geol Env 79(7):3289–3305
Wu JC, Xue YQ (2009) Groundwater dynamics. China Water Power Press, Beijng
Xiao CL, Liang XJ, Wang B (2009) Hydrogeology. Tsinghua University Press, Beijng
Xie ZF, Shen SL, Arulrajah A, Horpibulsuk S (2019) Environmentally sustainable groundwater control during dewatering with barriers: a case study in Shanghai. Undergr Space 6(1):12–23
Xu Z, Wang X, Li S, Gao B, Shi S, Xu X (2019) Parameter optimization for the thickness and hydraulic conductivity of tunnel lining and grouting rings. KSCE J Civ Eng 23(6):2772–2783
Yang G, Wang X, Wang X, Cao Y (2014) Analyses of seepage problems in a subsea tunnel considering effects of grouting and lining structure. Mar Georesour Geotechnol 34(1):65–70
Yang P, Zhao J, Li L (2021) An artificial freezing technique to facilitate shield tail brush replacement under high pore-water pressure using liquid nitrogen. KSCE J Civ Eng 5:1504–1514. https://doi.org/10.1007/s12205-021-0936-6
Ying HW, Zhu CW, Gong XN (2016) Analytic solution on seepage field of underwater tunnel considering grouting circle. J Zhejiang Univ (Engineering Science) 50(6):1018–1023
Ying HW, Zhu CW, Shen HW, Gong XN (2018) Semi-analytical solution for groundwater ingress into lined tunnel. Tunn Undergr Space Technol 76:43–47. https://doi.org/10.1016/j.tust.2018.03.009
Yoo C (2016) Ground settlement during tunneling in groundwater drawdown environment—Influencing factors. Undergr Space 1(1):20–29
Zhang YT (2003) Discussion on external hydraulic pressure upon rock tunnel lining. Mod Tunn Technol 40(3):1–4
Zhang ZD (2006) Semi-theoretical derivation for the formulas of water inflow and water pressure acting on a tunnel and their application to the waterproofing and drainage of tunnels. Mod Tunn Technol 43(1):1–7
Zhang XM, Jiang ZM, Feng SR, Chen SH (2011) Study on the determination of permeability coefficient of fractured rock mass under high pressure test condition. Hydroelectr Eng 30(1):155–159
Zhang W, Dai BB, Liu Z, Zhou CY (2019) On the non-Darcian seepage flow field around a deeply buried tunnel after excavation. Bull Eng Geol Env 78:311–323. https://doi.org/10.1007/s10064-017-1041-4
Zhang Z, Chen B, Li H, Zhang H (2022) The performance of mechanical characteristics and failure mode for tunnel concrete lining structure in water-rich layer. Tunn Undergr Space Technol 3:121. https://doi.org/10.1016/j.tust.2021.104335
Zhang J, Du R, Zhang X, Huang Z, Zhang W (2024) The deformation and failure characteristics of tunnels in layered rock with gentle dip angles after freeze–thaw cycles: Physical model tests and numerical investigation. Tunn Undergr Space Technol 144:105527
Zhao L (2017) Study on waterproof and drainage technology of mountain tunnel in high pressure and rich water area based on blocking groundwater and limiting discharge. Southwest Jiaotong University, Chengdu
Zhao QC (2018) Study on mechanical characteristics and waterproof and drainage technology of lining structure of large section highway tunnel in high pressure and rich water area. Southwest Jiaotong University, Chengdu
Zhou YF, Su K, Wu HG (2014) Study of external water pressure estimation method for reinforced concrete lining of hydraulic tunnels. Rock Soil Mech 35(S2):198–210

Zhou ZF, Huang Y, Fu ZM, Chen J, Wang JG (2015) The external water pressure on a deep buried tunnel in fractured rock. Tunn Undergr Space Technol 48:58–66

Zuo JP, Wu GS, Du J et al (2022) Rock strata failure behavior of deep ordovician limestone aquifer and multi-level control technology of water inrush based on microseismic monitoring and numerical methods. Rock Mech Rock Eng 55:4591–4614. https://doi.org/10.1007/s00603-022-02891-y